Journal of King Saud University – Science 34 (2022) 102017

Contents lists available at ScienceDirect

Journal of King Saud University – Science

journal homepage: www.sciencedirect.com

Original article

Green synthesis of palladium nanoparticles using aqueous plant extracts and its biomedical applications

S. Vinodhini [a,*], B. Scholastica Mary Vithiya [a,*], T. Augustine Arul Prasad [b]

[a] Department of Chemistry, Auxilium College (Affiliated to Thiruvalluvar University, Serkkadu, Vellore 632115), Vellore 632006, Tamil Nadu, India
[b] Department of Chemistry, Dwarakadoss Goverdhandoss Vaishnav College (Affiliated to University of Madras), Chennai 600106, Tamil Nadu, India

ARTICLE INFO

Article history:
Received 2 January 2022
Revised 25 March 2022
Accepted 5 April 2022
Available online 9 April 2022

Keywords:
Basella alba
Allium fistulosum
Tabernaemontanadivaricate
Green synthesis
Antimicrobial activity
Antifungal
Palladium nanoparticles

ABSTRACT

In recent years, metallic nanoparticles manufactured by green method have become a popular environmentally beneficial technology. Our current study describes an eco-friendly, biological production of palladium nanoparticles (PdNPs) with leaf extracts from *Allium fistulosum, Basella alba* and *Tabernaemontana divaricate*. Fourier transform infrared spectroscopy (FTIR), Ultraviolet–visible (UV–vis) spectroscopy, scanning electron microscopy (SEM), X-ray diffraction (XRD) and transmission electron microscopy (TEM) be used to characterise the produced PdNPs. The results of our SEM examination showed spherical form with a size of of 500 nm, 2 μm and 2 μm, correspondingly, for leaf extracts of *Allium fistulosum*, *Basella alba*, and *Tabernaemontana divaricate* derived PdNPs. In TEM images of all three extracts, the diameter and shape of the generated PdNPs were rather constant. Therefore, PdNPs with diameters ranging from 2 to 5 nm were measured respectively. Finally, all the extracts were evaluated for antioxidant, antifungal and antibacterial activity. The optimized PdNPs were taken for the application of dye degradation process by varying the concentration from 0 to 50 of different aliquots of PdNPs dispersions at different time of 0 to 10 and about 1 mL of congo red ($1x10^{-4}$ M) was mixed with 0.25 mg of PdNPs and kept for continuous stirring at room temperature (RT). The data demonstrated that the effects of duration and concentration were strongly related to the generated functional groups as well as nanoparticles, played an important role in decreasing metal ions and stabilising PdNPs in an environmentally manner.

1. Introduction

Nanomaterial improvement, especially of high quality, is a hot topic in nanoscience and technology these days. Metal techniques have sparked renewed attention due to its fascinating physical, thermodynamic and chemical properties, make great candidates for various applications such as optical electronics, catalysis, and biomedical applications (Azizi et al., 2017; Mani et al., 2021; Parasuraman et al., 2019; Sathiyaraj et al., 2021; Anju et al., 2019). Palladium nanoparticles, commonly known as PdNPs catalysts, have gained a lot of attention because of its useful uses in bioscience, biomedicine, and pharmacy. Because of its increased *surface-to-volume* ratio and enormous external strength, progress in the manufacture of Pd nanoparticles has gained tremendous relevance due to its use in both homogeneous and heterogeneous catalysis (Dauthal and Mukhopadhyay, 2013; Fahmy et al., 2020; Fahmy et al., 2020; Ghosh et al., 2015; Kapdi and Fairlamb, 2014). Electrical and chemical laser pulse ablation, and sonochemical decline procedures are common formulated PdNPs delivery methods. Because the synthetic chemical approaches used to make PdNPs have a punitive effect and reduce palladium's catalyst performance, new synthetic procedures are needed to fulfil a wide variety of possible purposes for the production of PdNPs with regulated size thickness. Metal ions can be reduced to NPs by physio-chemical, enzymatic, and biological processes (Liu et al., 2016; Mittal et al., 2013; Mohana and Sumathi, 2020; Nugroho et al., 2016; Rabiee et al., 2020). Higher radiation and concentrated reduction compounds are used in physio-chemical procedures, polluting the atmosphere and perhaps harming people's health. Nonetheless, the enzymatic approach of nanoparticle processing is superior, although it is more expensive. Due to a need to construct nature-friendly techniques in the processing of nanomaterials, the use of

* Corresponding authors.
E-mail addresses: vinodhinisanjeevee@gmail.com (S. Vinodhini), schol2005@auxiliumcollege.edu.in (B. Scholastica Mary Vithiya).
Peer review under responsibility of King Saud University.

Production and hosting by Elsevier

https://doi.org/10.1016/j.jksus.2022.102017
1018-3647/

biological processes has developed in the recent decade as a new and dependable technique for generating nanomaterials (Parasuraman et al., 2019; Ramesh et al., 2021; Badineni et al., 2021). The biosynthesis of metal NPs using tiny organisms and flora has taken a lot of time and effort. The plant absorbs and stores the metal atom's minimising qualities in a synthesis of NPs because it carries the metal atom's minimising properties. Because accuracy and highly developed structures are required, differences in the dimension and thickness of NPs generated by particular floras due to changes in the propagation and position of metal-based ions impair their qualities and restrict their usage (Nithiyavathi et al., 2021; Ramesh et al., 2021; Saldan et al., 2015; Saldan et al., 2015). Leaf extract, rather than whole plants, can be used to address these difficulties and obtain more control over their output and purification. A one-step biological reduction technique using flower extracts is the most straightforward method for dealing with ecologically friendly nanoparticles. Floral-based nanomaterial processing has received a lot of attention because of its rich biological diversity and ease of access. Floral crude aqueous extracts have been found to include novel 1° and 2° metabolites, which considerably reduce ionic metal form into environmentally beneficial nano-sized metallic nanoparticles. Nanoparticles made from leaf extracts have been used in a variety of therapeutic, nutritional, waste H_2O treatment, and cosmetic applications. Floral-based NPs have been successfully used as antimicrobials, larvicides, and cytotoxic agents in a number of studies. In light of these literary works, a biosynthetic technique based on plant resources has emerged as a viable and acceptable alternative to the physicochemical method currently in use. PdNPs have been described in present time publications using floral extract from a variety of plants, including *Basella alba*, *Allium fistulosm*, and *Tabernaemontana divaricate*. Still, the potential of floral resources must be investigated. *Basella alba (Basellaceae)* is a fast-growing, tasty perennial plant that can grow up to 9 m in length. *Tabernaemontana divaricate* and *Allium fistulosm,* for example, are flowering plants from the *Apocynaceae* and *Alliaceae* families, respectively. Antioxidant, antimicrobial, and anti-inflammatory properties were found in the extracts of all three plants (Salem and Fouda, 2021; Thakkar et al., 2010). The biogenic synthesis of PdNPs using several leaf extracts, including *Basella alba, Allium fistulosm,* and *Tabernaemontana divaricate,* is examined in this work. UV–vis, XRD, FTIR, SEM, as well as TEM spectroscopy were used to characterise the treated PdNPs. Pd NPs were also tested for antimicrobial, antifungal, and antioxidant properties were reported in detail.

2. Materials and methods

The three plants chosen for our studies are (i) *Tabernaemontanadivaricata*, (ii) *Basella alba, (iii)* Alliumfistulosum. Basella *alba* and *Alliumfistulosum* were collected from the Karadikudi village agricultural farm, while *Tabernaemontan adivaricata* were collected from the Vellore area.

2.1. Preparation of plant extract

The leaves were properly washed to eliminate dust and fungal spores, and then shade dried to remove moisture. On the heating mantle, about 10 g of *Basella alba* leaves were put to a 250 mL beaker containing 200 mL distilled water and cooked for 45 min. The extract was cooled to room temperature before being filtered. The extracts of the other two plants, namely *Tabernaemontanadivaricata* and *Alliumfistulosum* were also similarly prepared.

2.2. Synthesis of palladium nanoparticles

Precursors for PdNPs synthesis were palladium acetate solution. *Basella alba, Alliumfistulosum*, and *Tabernaemontanadivaricata* aqueous extracts were introduced in varying amounts to test tubes containing 2 mM aqueous palladium acetate solution. The creation of PdNPs were detected by a change in the colour of the solution. When *Tabernaemontanadivaricata* leaf extract and *Alliumfistulosum* leaf extract were applied dropwise to palladium acetate, the colour changed from mild brown to dark brown, indicating the creation of palladium nanoparticles. The colour of *Basella alba* has changed from pale brown to green. The excitation of surface plasmon vibrations causes the colour shift in aqueous solution.

3. Characterisation of palladium nanoparticles

3.1. UV–vis spectral analysis

By using a twin beam UV–visible spectrophotometer with multiple wavelengths spanning from 200 to 1000 nm, the reduction of palladium ion to metallic PdNPs were spectroscopically determined. After experimenting with different palladium acetate concentrations, the best conditions for processing palladium NPs from extracts were discovered to be 2 mM palladium acetate at 60 °C. Based on time of reaction, the UV–vis intensity was steadily increased to a constant level. Due to the stimulation of surface plasmon resonance in a PdNPs, the colour shifts from light to dark brown and mild brown to green. Using a Varian Cary-50 UV–visible absorption spectrophotometer, these optic-based features of PdNPs were investigated.

3.2. Fourier transform infrared spectroscopy (FTIR)

FTIR (Varian 800) was used to determine the functional group of produced PdNPs, which was compared to aqueous extracts of *Basella alba, Allium fistulosum*, and *Tabernaemontana divaricate*. To make the pellet, the synthesised samples were assorted by potassium bromide (KBr) in a ratio of 1:99, followed by scan in between 400 and 4000 cm^{-1} within a resolution of 2 cm^{-1}.

3.2.1. X-ray diffraction (XRD)

Using X'Pertpro, the XRD technique was used to determine the crystal's dimension. Analytical X-ray 107 diffraction with copper potassium (alpha) radiation is 10° to 80°.

3.3. Scanning electron microscopy (SEM)

Crystal-like nature and dimension of the PdNPs were further verified by using a SEM configuration for PdNPs that showed evidence of palladium metal material.

3.4. Transmission electron microscopy (TEM)

The transmission electron microscope is used to examine the shape, size, and structure of PdNPs. On the carbon-coated copper grid, a single droplet suspension of PdNPs were inserted. From the collected TEM images, an imageJ platform is used to determine the dimension and shape of PdNPs.

3.5. Antimicrobial study

The antibacterial activity of PdNPs produced from *Basella alba, Allium fistulosum, and Tabernaemontana divaricate* were studied using the well diffusion approach. As test organisms, bacteria such as E. coli, Staphylococcus aureus, Bacillus cereus, Bacillus subtilis,

along with Enterobacter cloaca were used. The strains were transferred to petri plates on the outside of a germ-free nutrient agar medium after 24 h of growth. In each plate, a total of three wells with a diameter of 5 mm were filled with 10 µl, 25 µl, 50 µl and 100 µl of samples and 50 µl of PdNPs (1 mg/mL), distilled H_2O, and an antibiotic disc (Gentamicin sulphate) as a reference. Furthermore, these plates were kept at room temperature for 24 h, and the zone of inhibition was studied for each bacteria trial.

3.6. Antioxidant study

3.6.1. DPPH radical scavenging activity

The 2, 2-diphenyl-1-picrylhydrazyl method were used to measure plant extract the free radical scavenging activity in water as a solvent (DPPH). Free radical scavenging activity of DPPH was tested using the procedure described. An aliquot of 3 mL of 0.004% DPPH solution in water was combined with 0.5 to 2.5 L of plant extract/ascorbic acid at varied doses. The mixture was briskly agitated and allowed to settle at room temperature. The absorbance at 518 nm of DPPH was measured using a UV–vis spectrophotometer to assess decolorization (LMSP-UV1000B). Instead of plant extract/ascorbic acid, 0.1 mL of the appropriate vehicle was used as a control. The absorbance values of experimental tubes and control are compared and the % suppression of DPPH radicals by the extract/compound was calculated.

$$Scvenging\ activity\% = \frac{A(control) - A(sample)}{A(control)} \times 100$$

3.6.2. Anti-fungal study

The antifungal activity of QDP generated PdNPs is identified using well diffusion method in this study. The test organisms were *Candida albicans, Aspergillus flavus*, and penicillium sps, which are all fungal strains. Under sterile conditions, fresh potato dextrose agar (PDA) plates were spread plated with test organisms. Each plate's agar was pierced with three 6 mm wells, which were aseptically filled with 50 mL of the nanoparticle solution. The plates were incubated in the dark at 25 °C for 1, 2, 4, and 7 days before being inspected. Each well's inhibition of fungal growth was measured three times and the average were calculated.

3.6.3. Antidiabetic activity

α-amylase inhibition activity of acarbose, **V, N** and **P** at different concentrations.

Anti diabetic assay:alpha-amylase: the starch-iodine technique was used to measure alpha-amylase activity. 10 L of -amylase solution (0.025 mg/mL) were combined with 390 L of phosphate buffer

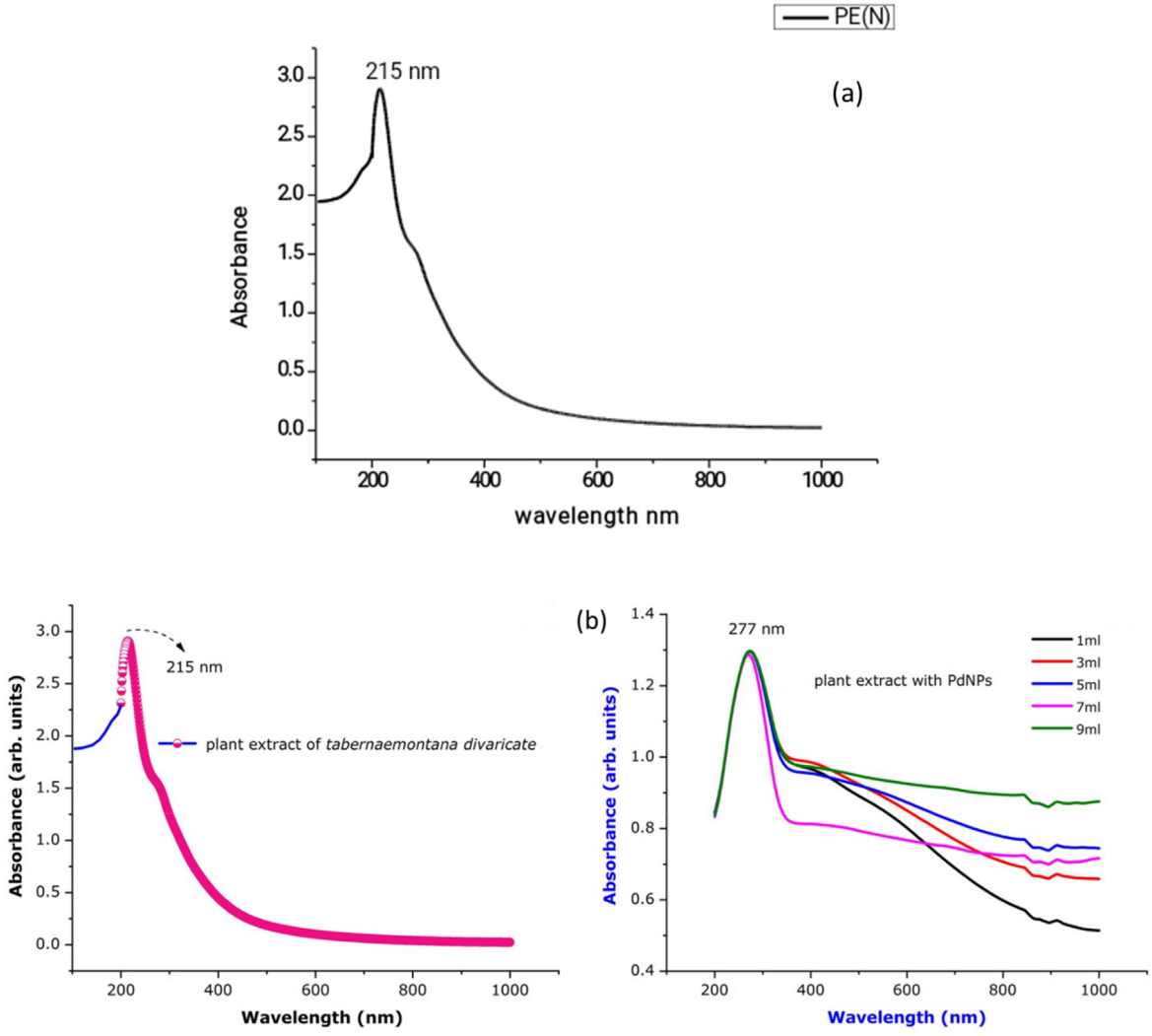

Fig. 1. UV–visible spectral study of (a) Plant extract of *Tabernaemontanadivaricata;* (b) PdNPs with *Tabernaemontanadivaricata.*

(0.02 M containing 0.006 M NaCl, pH 7.0) having various extract concentrations. After a 10-minute incubation at 37 °C, 100 L of 1% starch solution was added, and the mixture was re-incubated for 1 h. After that, 0.1 mL of 1 percent iodine solution was added, followed by 5 mL distilled water, and the absorbance was measured at 565 nm. The same reaction conditions were used to determine the sample, substrate, and -amylase blank. The amount of enzyme activity that was inhibited was determined as;

$$\%\,\textbf{Inhibition} = \frac{\textit{Absorbance of control - Absorbance of sample}}{\textit{Absorbance of control}}$$

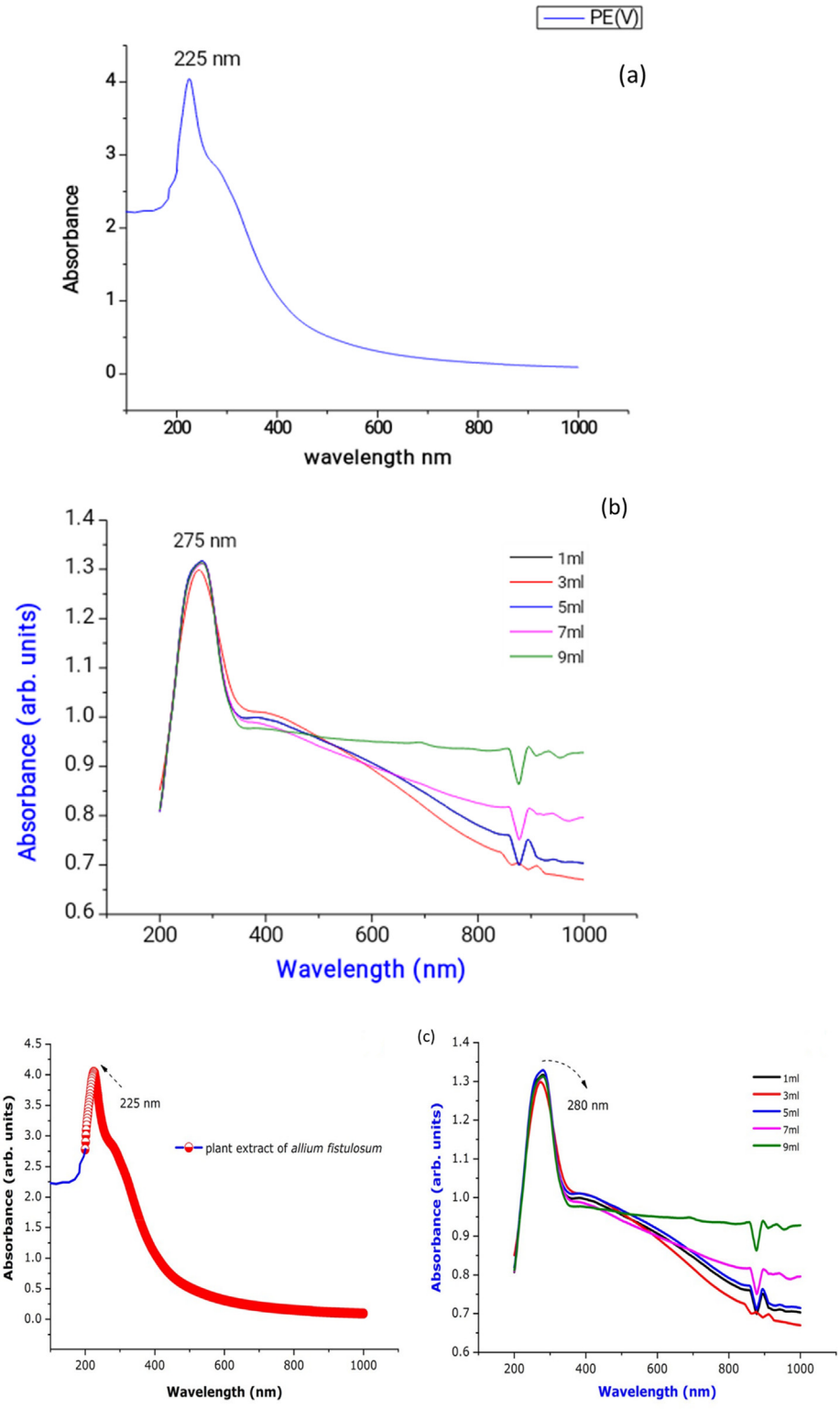

Fig. 2. UV–visible spectral study of (a) plant extract of *Alliumfistulosum* (b) Pd nanoparticles (c) PdNPs with *Alliumfistulosum.*

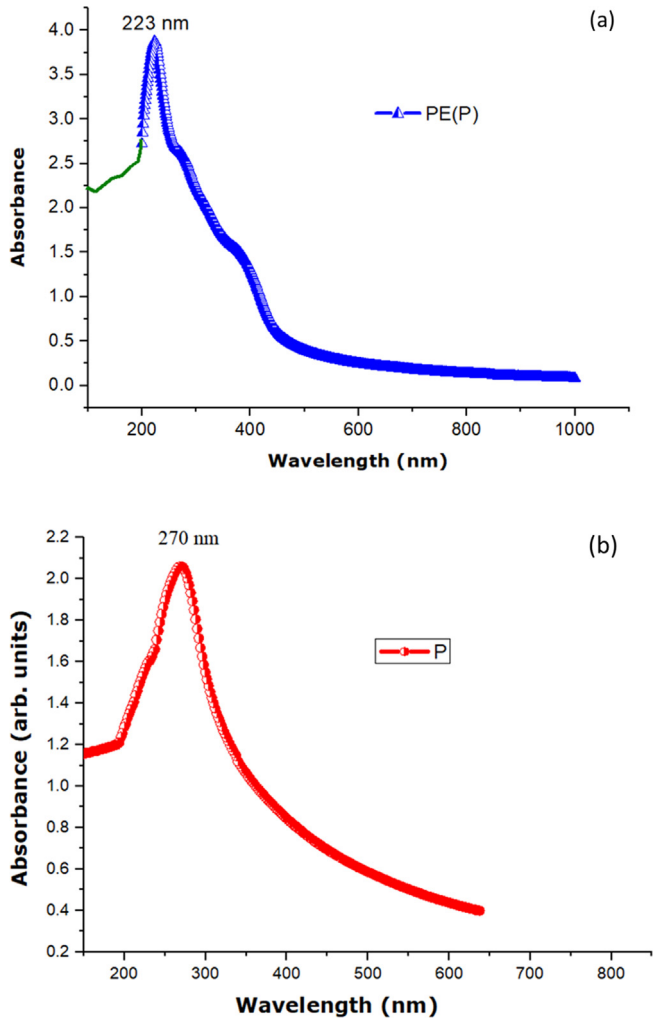

Fig. 3. UV–visible spectral study of (a) plant extract of *Basella alba* (b) PdNPs with *Basella alba.*

3.6.4. Catalytic activity of PdNPs

The catalytic activity of as-generated PdNPs for the selective oxidation of benzyl alcohol was investigated in order to investigate the potential application of green synthesised PdNPs in the field of catalysis.

3.6.5. Benzyl alcohol oxidation

The catalytic activity of Pd nanoparticles produced with varying amounts (1, 5, and 10 mL) of plant extract as an oxidation catalyst was tested. The reaction mixture was collected every 10 min and quenched immediately to evaluate the reaction's kinetics, which were then studied using a capillary column and gas chromatography (GC). The following was the GC methodology for the kinetic investigation and product analysis: The column was initially heated to 120 °C, then elevated to 180 °C at a rate of 100 °C min^{-1} and maintained at this temperature for 10 min. The status of the reaction was determined and the results were acquired using this process.

3.7. Photocatalytic behaviour

The dye deprivation investigation was carried out using the biologically produced PdNPs. 2 mL of eppendorf vial was used to keep the reaction mixture. 0.25 mg of PdNPs were added to nearly 1 mL of congo red dye, pH levels ranged from 2 to 10. The aliquot parts were shaken for 1 h at room temperature in a rotary shaker. Following the incubation period, the specimen was centrifuged at 1000 rpm. A UV–vis spectrometer was used to determine the amount of leftover dye in the supernatant.

3.8. Results and discussion

3.8.1. UV–vis spectral analysis

The results of UV–visible spectrum analysis provide a 1° insight into the production of nanoparticles. Under UV–visible spectroscopy, a three-group of plant extracts, including *Basella alba, Allium fistulosum,* and *Tabernaemontana divaricate* coupled with palladium nanoparticles, were examined as shown in Fig. 1.

A double beam UV–visible spectrophotometer was used to identify the reduction of palladium ion to metallic PdNPs at different wavelengths spanning from 200 to 1000 nm. UV–visible spectroscopy was used to examine three plant extracts: *Tabernaemontana divaricata, Basella alba,* and *Allium fistulosum* in combination with palladium nanoparticles. PdNPs were produced using a plant extract from *Tabernaemontana divaricata.* The maximal absorption peak of PdNPs is 215 and 277 nm, respectively. PdNPs are formed as seen by the significant hump. Similarly, a comparison of extracts of *Allium fistulosum* and *Basella alba* with Pd nanoparticles as shown in Fig. 2. *Allium fistulosum* and *Basella alba* extracts had absorption peaks of 225 nm and 223 nm, respectively. Their produced PdNPs, on the other hand, had peak intensities of 275 nm and 270 nm, respectively. Surface plasmon resonance, which is an inherent property of metal-based NPs, caused the colour shift as shown in Fig. 3. In comparison to crude plant extracts, the peak in PdNPs showed a significant improvement. Overall, the UV spectrum examination of the PdNPs shows an increase in the absorption peak, indicating that palladium nanoparticle creation is becoming more substantial.

3.8.2. FTIR spectral study of biosynthesized PdNPs

FTIR analysis was used to find absorption peaks in both NPs and floral extracts, with PdNPs being assigned to symmetry and antisymmetry frequency of broadening. Fig. 4 shows the results for all three palladium nanoparticle extracts. A spectrum of *Tabernaemontanadivaricate* produced particles, shown in Fig. 4(a), revealed a total of three peaks, with the most influential peak at 1070 cm^{-1}, and minor peaks at 1554 and 1411 cm^{-1}, respectively. Fig. 4(b) shows a spectrum of an *Allium fistulosum* - synthesised particle with three peaks, the most prominent of which is at 1121 cm^{-1} with minor peaks at 1457 and 1599 cm^{-1}, respectively. A spectrum of *Basella alba* generated particles, shown in Fig. 4(c), revealed three peaks, with the most prominent peak at 1108 cm^{-1} and smaller heights at 1618 and 2987 cm^{-1} respectively.

3.8.3. XRD analysis

Fig. 5(a-c) indicate the crystallinity and stages of biologically produced PdNPs based on XRD spectral analysis 5(c). The spectra of *Tabernaemontana divaricate* PdNPs extract in Fig. 5(a) has two peaks at 40°, 50.2°, 60.3°, and 70.8°, confirming the presence of 39.515, 51.583, 61.395, and 77.365 groups of Bragg's reflection lattice planes, respectively. Similarly, as shown in Fig. 5(b), an arrangement of Pd nanoparticles synthesised using *Allium fistulosum* (2 values of 50° and 38° that confirms the presence of 39.302, 51.495, 61.235, and 77.320 groups) and *Basella alba* (2 values of 30.8°, 50°, 59.9°, and 78.7° that confirms the presence of 36.707, 49.060, 58.480, and 74.8 (c).

3.8.4. Electron microscopy analysis (SEM & TEM)

PdNPs made from *Basella alba, Allium fistulosum,* and *Tabernaemontana divaricate,* as seen under a scanning electron microscope. For the extracts of *Basella alba, Allium fistulosum,* and *Tabernaemon-*

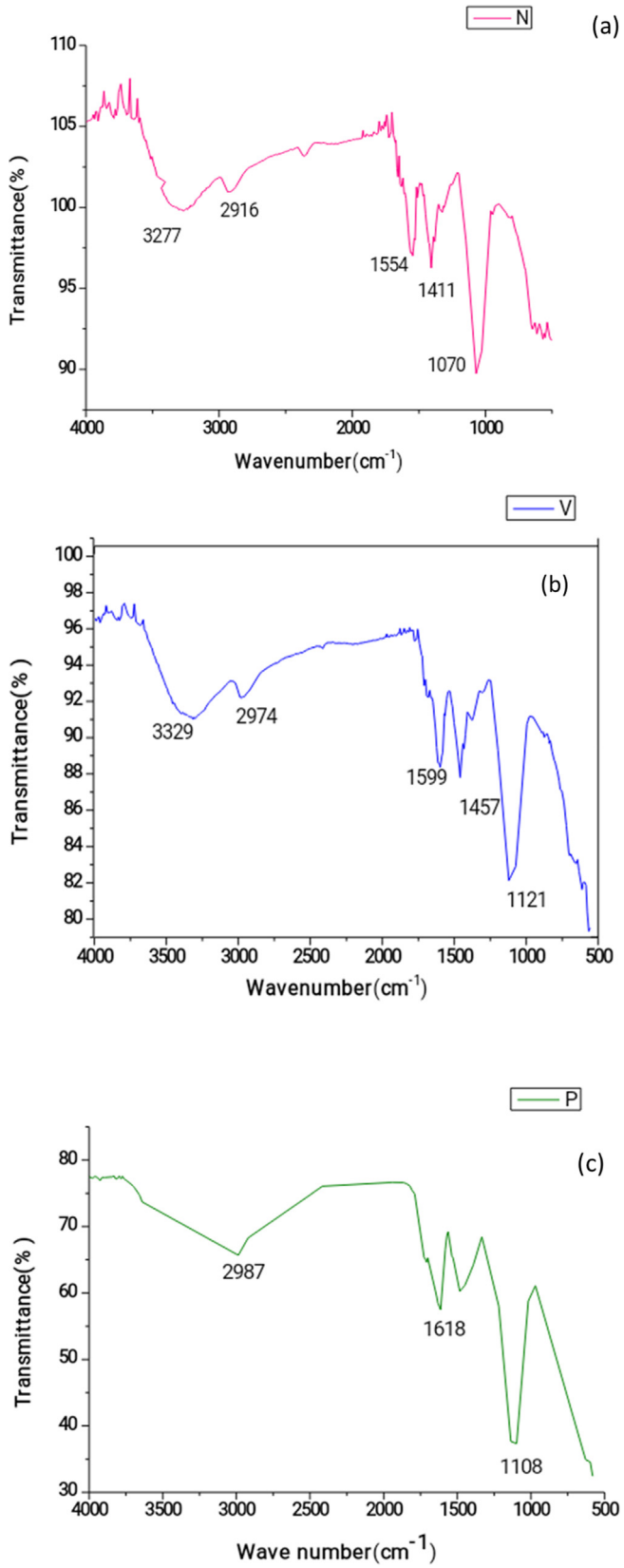

Fig. 4. (a) *Tabernaemontana divaricate*; (b) Pd NPs with *Alliumfistulosum* and (c) Pd NPs with *Basella alba.*

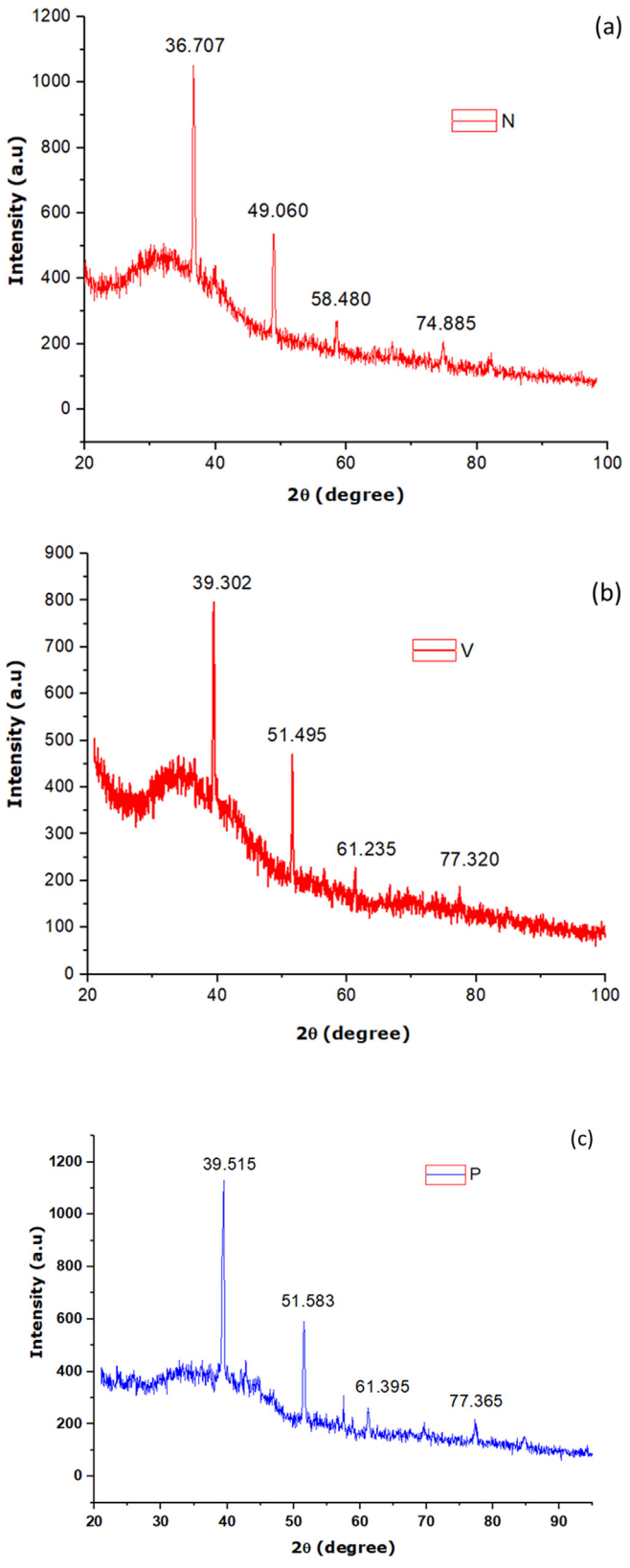

Fig. 5. XRD diffraction pattern of synthesized Pd NPs (a) *Tabernaemontana divaricate* extract, (b) Pd NPs with *Allium fistulosum*and (c) Pd NPs with *Basella alba.*

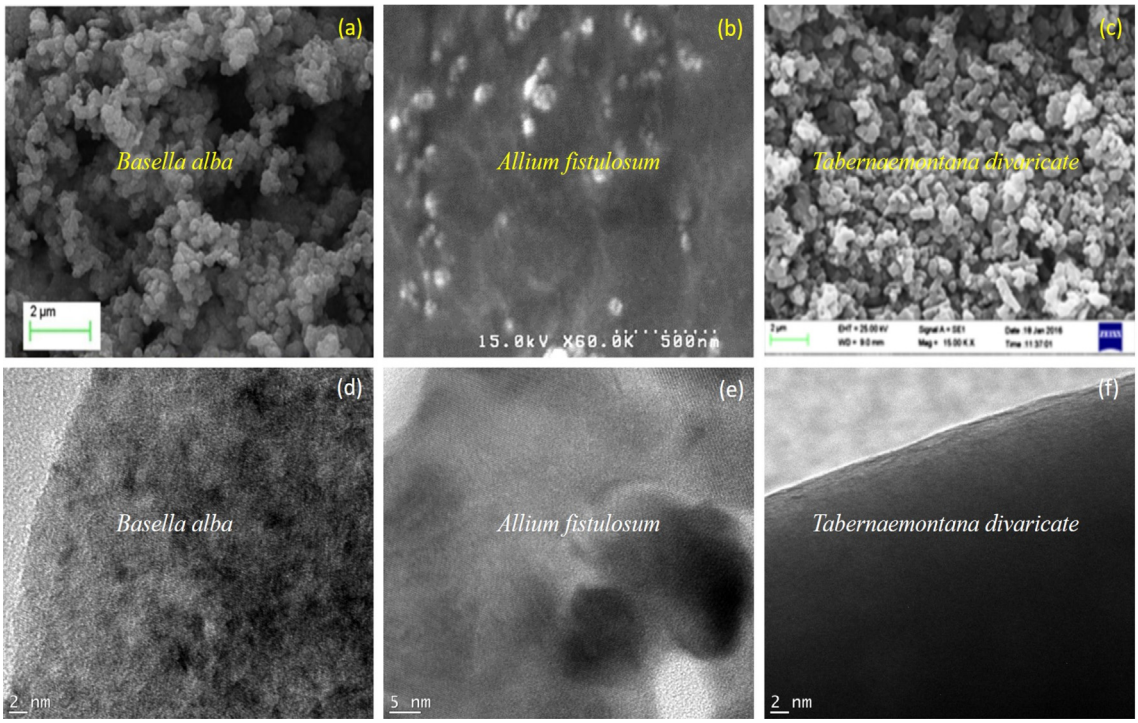

Fig. 6. SEM and TEM image of synthesized Pd nanoparticles.

tana divaricate produced palladium nanoparticles, our examination revealed spherical morphology with dimensions of 2 µm, 500 nm, and 2 µm, respectively in SEM images in Fig. 6. When compared to the other two extracts of processes nanoparticles, the palladium nanoparticle created from the extract of *Allium fistulosum* was determined to be superior. The diameter and shape of produced PdNPs were reasonably consistent in TEM images of all three extracts. PdNPs were measured in the 20 to 50 nm range. The *Tabernaemontana divaricata* extract was shown to be appropriate and effective for producing highly stable PdNPs in TEM experiments. TEM was used to investigate particle size, shape, and crystallinity.

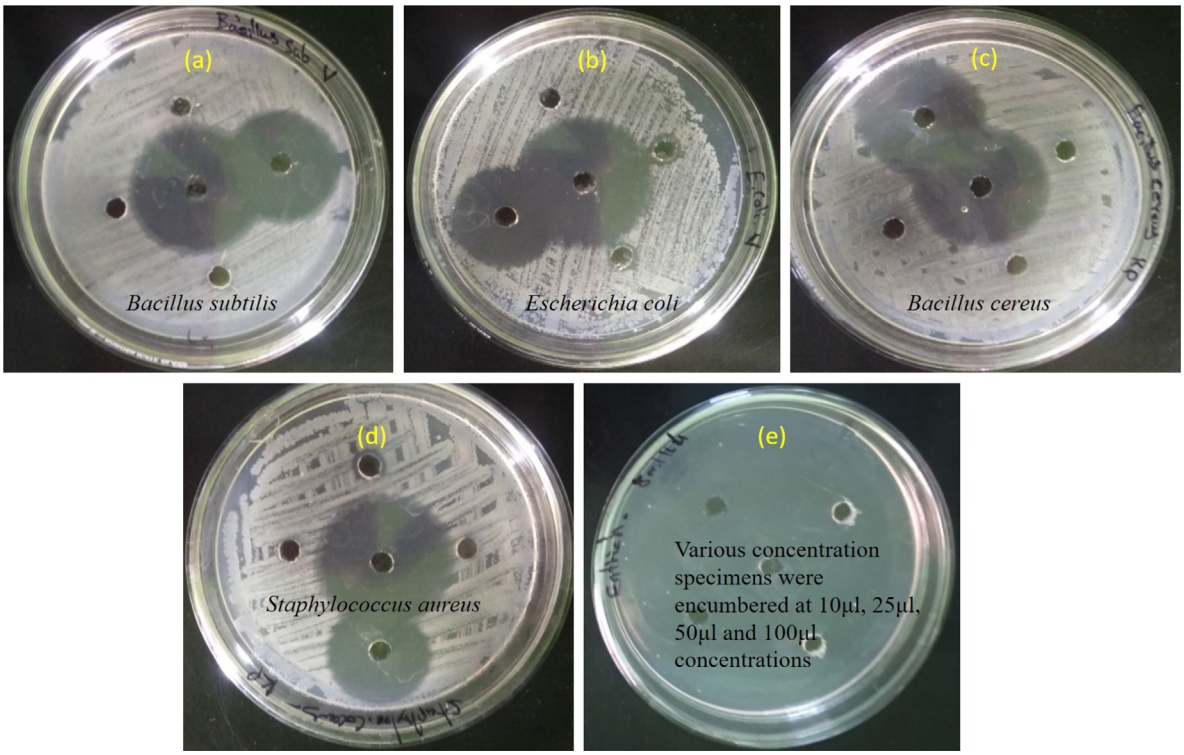

Fig. 7. Zone of inhibiton of various bacterias (a) *Bacillus subtilis* (b) *Escherichia coli* (c) *Bacillus cereus* (d) *Staphylococcus aureus* (e) various concentration specimens were encumbered at 10 µl, 25 µl, 50 µl and 100 µl concentrations.

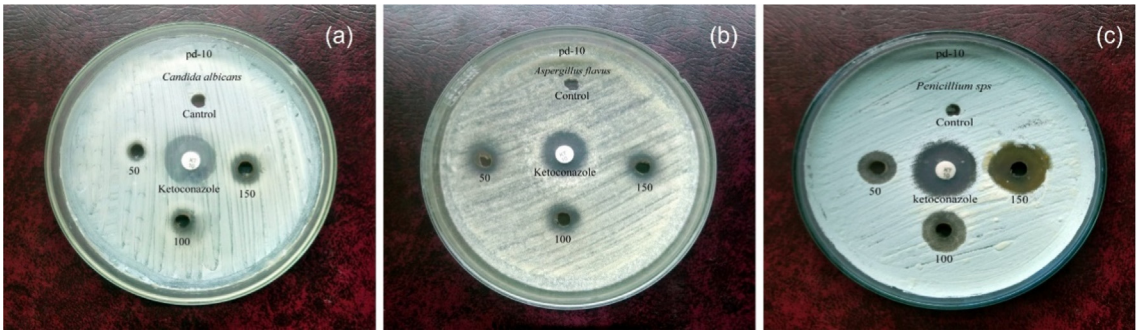

Fig. 8. Zone of inhibiton of various fungi (a) *Candida albicans* (b) *Aspergillus flavus* (c) *Penicillium sps.*

3.8.5. Antibacterial activity

Antimicrobial activity plates of various microbes.

Microorganism	Control - Gentamicin Sulphate	KP	V	N
	Zone of inhibition in mm			
Staphylococcus aureus	14 mm	11 mm	12 mm	9 mm
Escherichia coli	21 mm	18 mm	16 mm	13 mm
Bacillus subtilis	25 mm	14 mm	17 mm	18 mm
Bacillus cereus	26 mm	20 mm	18 mm	15 mm
Enterobacter cloaca	–	–	–	–

In this report, the PdNPs exhibited stronger bactericidal activity towards *Escherichia coli*, *Staphylococcus aureus, Bacillus subtilis* and *Bacillus cereus* might be because of the point that PdNPs can simply enter within thinner outer layer speedily to suppress the metabolic action in comparison with the thicker sheath of the gram-positive microbes whereas it is not showing any activity against *Enterobacter cloaca.* Also, the various leaf extracts phyto-chemicals exist as capping material in the PdNPs exterior might affect the antimicrobial activity towards gram negative microbes. Moreover, diverse concentration specimens were encumbered in nutrient agar medium of well pates at a concentration of 10 µl, 25 µl, 50 µl and 100 µl values as shown in Fig. 7. The standard control specimen gentamicin sulphate is injected in every plates 10 µl at the center well. The highest zone range is depicted in a greater concentration at 100 µl KP, V, N in the well plates.

3.8.6. Antifungal activity

PdNPs were tested for antifungal activity against three different pathogenic fungus in this study *Aspergillus flavus, Penicillium sps,* and *Candida albicans.* In this investigation, three different PdNPs solutions were employed in Fig. 8. For solutions 1 through 3, the average diameters were 50 nm, 100 nm, and 150 nm, respectively.

S. NO	Microorganisms	Control	Pd			Ketoconazole
			50	100	150	
		Zone of inhibition in mm				
1.	*Candida albicans*	–	06	07	10	18
2.	*Aspergillus flavus*	–	12	13	14	20
3.	*Penicilliumsps*	–	12	15	18	19

3.8.7. Antioxidant activity

The anti-oxidant action of produced PdNPs were evaluated by DPPH procedure. In DPPH steady natural free radical which was

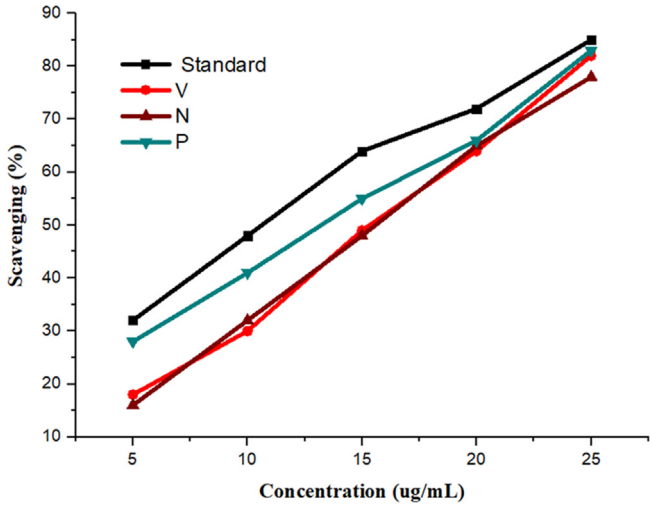

Fig. 9. Antioxidant activity of synthesized Pd nanoparticles.

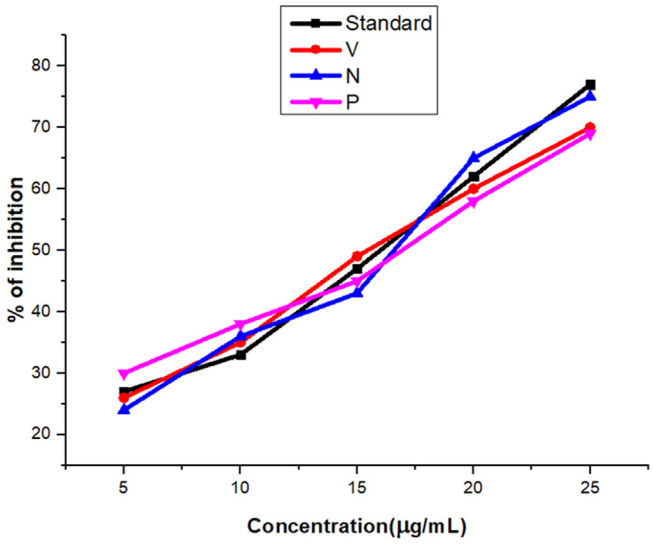

Fig. 10. Antidiabetic activity of PdNPs using V- *Allium fistulosum*,N-*Tabernaemontanadivaricata*,P- *Basella alba.*

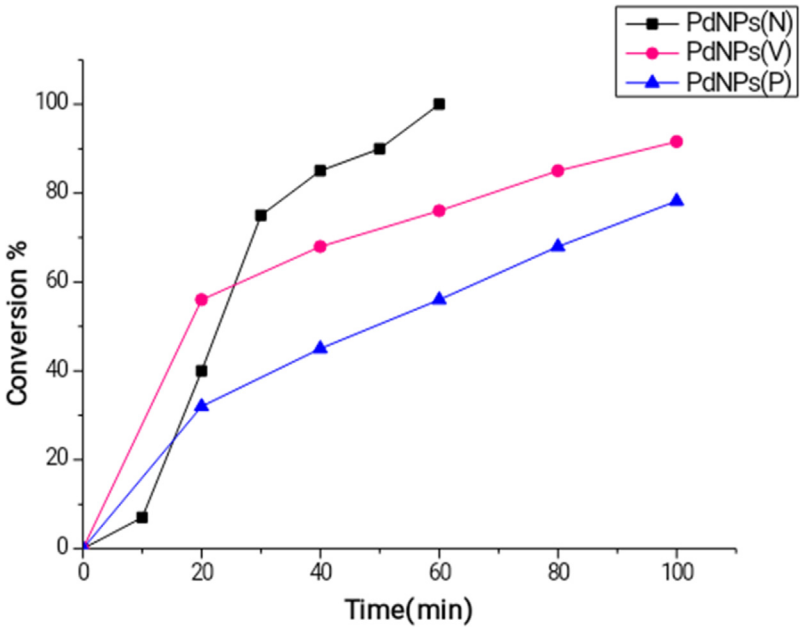

Fig. 11. Catalytic activity of Pd nanoparticles.

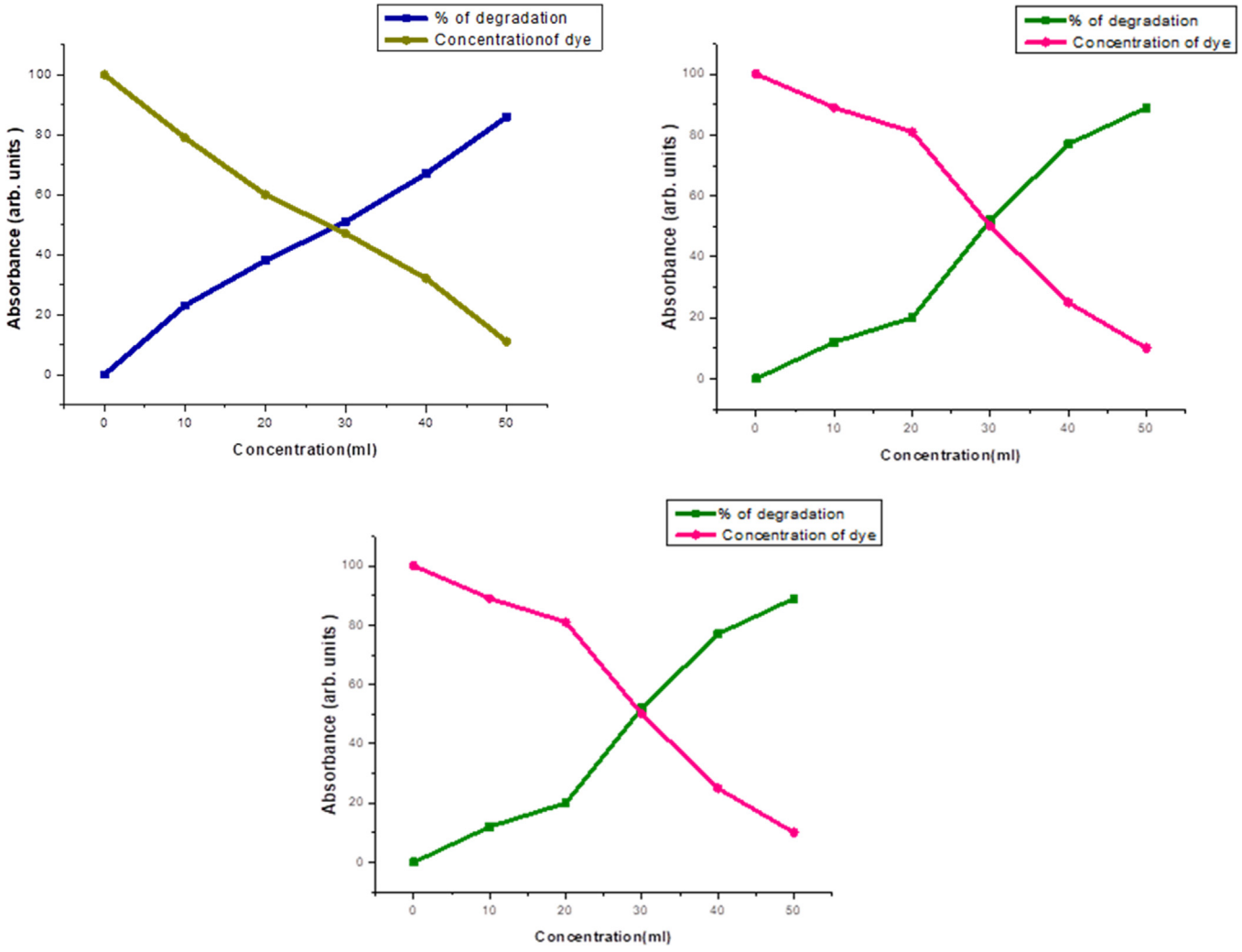

Fig. 12. Photocatalytic activity of Pd NPs at 50 μg concentration.

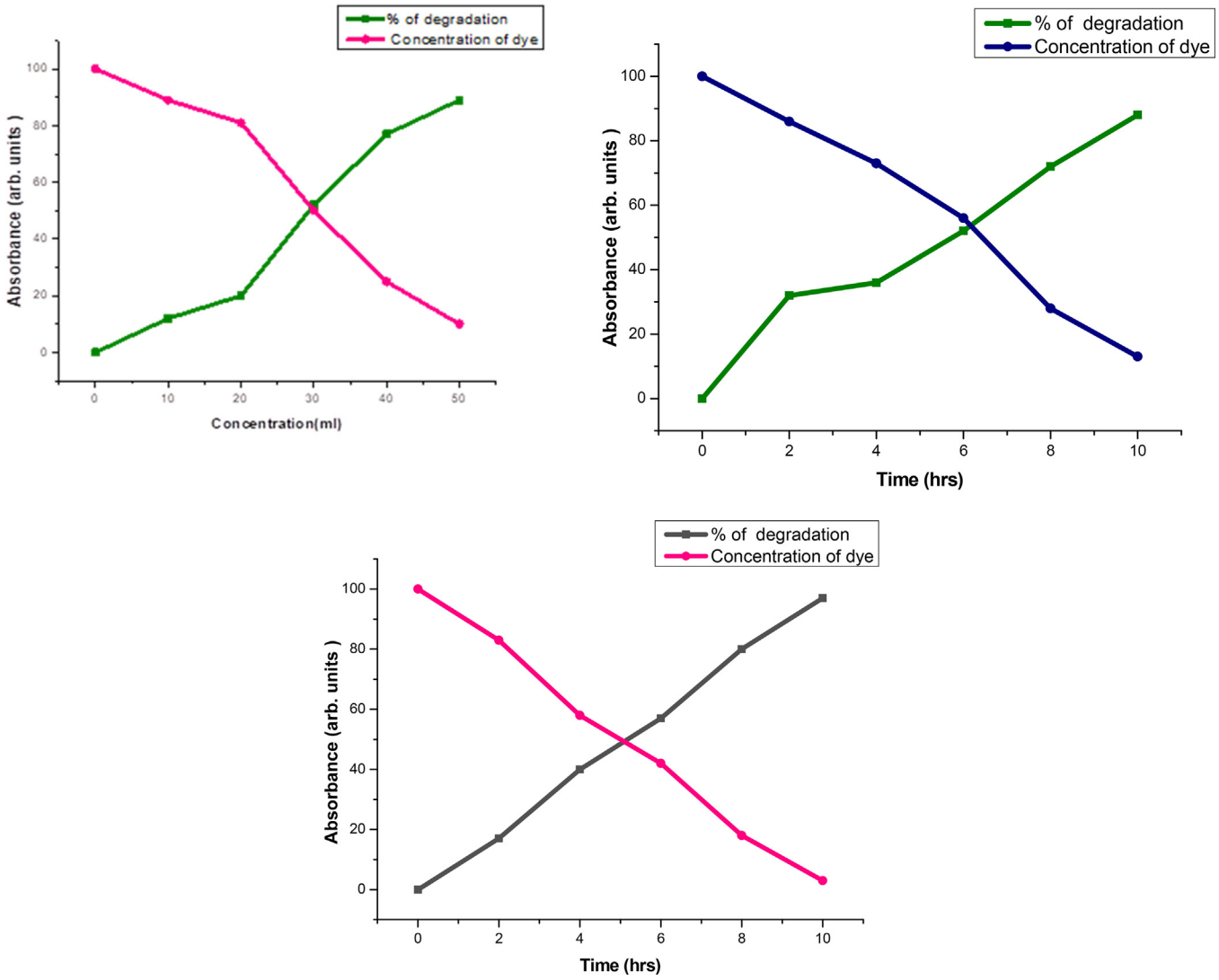

Fig. 13. Photocatalytic activity of Pd NPs at time in 10 hr.

employed for examining the free radical actions and then antioxidant action of numerous organic substances. Different concentration of each samples such as 200, 400, 600, 800, and 1000 μg were used for the antioxidant study. *Basella alba* mediated Pd nanoparticle showed higher inhibition percent at 1000 μg concentration compared to others. It also reveals that as the concentration enhances the percent suppression also enhances i.e, the percent inhibition was found to be 23–64% for the sample concentration 200–1000 μg. In Fig. 9 gives a clear idea that inhibition activity is a dose dependent activity.

3.8.8. Antidiabetic activity

Diabetes mellitus is a set of metabolic illnesses characterised by persistently elevated blood sugar levels. Inhibiting carbohydrate digesting enzymes (*-glucosidase and -amylase*) is one way to treat hyperglycemia by limiting the breakdown of carbohydrates into monosaccharides, which is a major cause of high blood glucose levels. As a result, creating drugs that inhibit carbohydrate hydrolysing enzymes could be an effective strategy to treat diabetes. The principal enzyme intricate in the interruption of polysaccharides and the proclamation of sugar into the bloodstream is alpha-amylase, that results in an increase in blood glucose levels and, eventually, diabetes. This enzyme's repressive impact may have a possible beneficial impact on diabetes. The materials were diluted into different concentrations such as 5, 10, 15, 20, and 25 g/mL in order to assess the antidiabetic property. Fig. 10 depicts the percent inhibitory impact of PdNPs on the enzyme. PdNPs showed a repressive impact on an enzyme in a dosage-based manner as well as when the dosage was enlarged to 25 μg/mL. It might be evaluated from the outcomes that PdNPs might act as a substitute due to its potent repressive impact which have on its enzyme. The result also suggests that PdNP synthesized using *Tabernaemontanadivaricata* showed higher inhibition compared to the Pd prepared from other two source such as *Basella alba* and *Allium fistulosum.* Around 80% of inhibition was found in PdNPs synthesized by *Tabernaemontanadivaricata*at the concentration of 25 μg/mL.

3.9. Catalytic activity

The catalytic action of three different extracts of Pd NPs were shown in Fig. 11 which was found as 60, 100 and 100 mins for *Tabernaemontana divaricate (N), Allium fistulosum* (V) and *Basella alba* (P) respectively. When the PdNPs were pre-processed by employing the 1 mL plant extract (V), the conversion by-product creation starts 10 min once the reaction get initiated and gradually proceeds against 100% conversion product that is benzaldehyde

was attained after 50 min of reaction period. Nevertheless, when PdNPs were made with 5 mL plant extract (N), the reaction kinetics were discovered to be differ from the formerly used method (V). The reaction begins with a conversion of 65 percent after 20 min, but it is terminated after 100 min, providing a maximum conversion of 93.6 percent, which is quite different from the previous catalyst, which yielded a 100 percent conversion product in 50 min. Likewise, the catalytic performance of PdNPs ready with 10 mL plant extract (P) was assessed. It was discovered that 20 min at the beginning of the reaction, 34% of the conversion product was developed, whilst at the end of 100 min, a maximum of 78.5 percent conversion product was procured, as well as the reaction was not proceeded further (Mangala Nagasundari et al., 2021; Thirupathy et al., 2020; Geetha et al., 2018; Amanulla et al., 2019; Subbareddy et al., 2020). Based on the foregoing findings, it can be concluded that the Pd nanoparticles made with 1 mL plant extract were of good quality produced a 100 per cent conversion product in 50 min of reaction period.

3.9.1. Photocatalytic activity

Figs. 12 and 13 shows the photocatalytic action of all the 3 extracts at a concentration (50 µg) and time (10 hr). The optimized Pd NP was taken for the application of dye degradation process by varying the concentration from 0 to 50 of different aliquots of Pd NPs dispersions at different time of 0 to 10 and about 1 mL of congo red ($1x10^{-4}$ M) was mixed with 0.25 mg of Pd NPs and kept for continuous stirring at room temperature (Alhaji et al., 2019; George et al., 2022; Magdalane et al., 2021; Amanulla et al., 2021; Kayalvizhi et al., 2022). The clear surface plasmon resonance (SPR) band for dye was observed in 433 nm. At pH 6 SPR band in 433 has been disappeared (Perumal et al., 2022; George et al., 2022; Ayeshamariam et al., 2021; Palem et al., 2022; Bathula et al., 2020; Mallikarjuna et al., 2019; Mallikarjuna et al., 2017).

4. Conclusion

Plant extracts such as *Allium fistulosum, Tabernaemontanadivaricata, and Basella alba* have been successfully used to synthesise Pd NPs in a lesser price, eco-friendly approach. UV, FTIR, XRD, TEM and SEM were used to characterise the synthesised Pd NPs. Biosynthesised Pd NPs are nontoxic and have antibacterial, antifungal, antioxidant, and anti-diabetic properties. Pd nanoparticles synthesised with Allium fistulosum (V-Ag) demonstrated a good zone of inhibition against both bacterial and fungal strains among the three sources of synthesis. When it comes to antioxidants and antidiabetics, research demonstrate that as concentration rises, so does action. Moreover, the catalytic and photocatalytic action of Pd NPs were also showed good superior activity. The findings are highly positive, demonstrating a significant increase in the activity of the undamaged fractions. The use of biological sources to synthesise nanoparticles adds a new dimension to all application areas.

Declaration of Competing Interest

The authors declare that they have no known competing financial interests or personal relationships that could have appeared to influence the work reported in this paper.

References

Azizi, S., Mahdavi Shahri, M., Rahman, H.S., Rahim, R.A., Rasedee, A., Mohamad, R., 2017. Green synthesis PdNPs mediated by white tea (Camellia sinensis) extract with antioxidant, antibacterial, and antiproliferative activities toward the human leukemia (MOLT-4) cell line. Int. J. Nanomed. 12, 8841–8853.

Mani, M., Harikrishnan, R., Purushothaman, P., Pavithra, S., Rajkumar, P., Kumaresan, S., Al Farraj, D.A., Elshikh, M.S., Balasubramanian, B., Kaviyarasu, K., 2021. Systematic green synthesis of silver oxide nanoparticles for antimicrobial activity. Environ. Res. 202.

Parasuraman, P., Anju, V.T., Sruthil Lal, S.B., Sharan, A., Busi, S., Kaviyarasu, K., Arshad, M., Dawoud, T.M.S., Syed, A., 2019. Synthesis and antimicrobial photodynamic effect of methylene blue conjugated carbon nanotubes on E. coli and S. aureus. Photochem. Photobiol. Sci. 18 (2), 563–576.

Sathiyaraj, S., Suriyakala, G., Dhanesh Gandhi, A., Babujanarthanam, R., Almaary, K. S., Chen, T.-W., Kaviyarasu, K., 2021. Biosynthesis, characterization, and antibacterial activity of gold nanoparticles. J. Infect. Public Health 14 (12), 1842–1847.

Anju, V.T., Paramanantham, P., Sruthil Lal, S.B., Sharan, A., Syed, A., Bahkali, N.A., Alsaedi, M.H., Kaviyarasu, K., Busi, S., 2019. Antimicrobial photodynamic activity of toluidine blue-carbon nanotube conjugate against Pseudomonas aeruginosa and Staphylococcus aureus-understanding the mechanism of action. Photodiagn. Photodyn. Ther. 27, 305–316.

Dauthal, P., Mukhopadhyay, M., 2013. Biosynthesis of PdNPs using delonix regia leaf extract and its catalytic activity for nitro-aromatics hydrogenation. Ind. Eng. Chem. Res. https://doi.org/10.1021/ie403410z.

Fahmy, S.A., Preis, E., Bakowsky, U., Azzazy, H.-M.-E.-S., 2020. PdNPs fabricated by green chemistry: promising chemotherapeutic, antioxidant and antimicrobial agents. Materials 13, 3661.

Fahmy, S.A., Preis, E., Bakowsky, U., Azzazy, H.-M.-E.-S., 2020. Platinum nanoparticles: green synthesis and biomedical applications. Molecules 25, 4981.

Ghosh, S., Nitnavare, R., Dewle, A., Tomar, G.B., Chippalkatti, R., More, P., Chopade, B. A., 2015. Novel platinum–palladium bimetallic nanoparticles synthesized by Dioscorea bulbifera: Anticancer and antioxidant activities. Int. J. Nanomed. 10, 7477–7490.

Kapdi, R., Fairlamb, I.J.S., 2014. Anti-cancer palladium complexes: A focus on PdX2L2, palladacycles and related complexes. Chem. Soc. Rev. 43, 4751–4777.

Liu, Y., Wang, D.-D., Zhao, L., Lin, M., Sun, H.-Z., Sun, H.-C., Yang, B., 2016. Polypyrrole-coated flower-like Pd nanoparticles (Pd NPs@PPy) with enhanced stability and heat conversion efficiency for cancer photothermal therapy. RSC Adv. 6, 15854–15860.

Mittal, A.K., Chisti, Y., Banerjee, U.C., 2013. Synthesis of metallic nanoparticles using plant extracts. Biotechnol. Adv. 31, 346–356.

Mohana, S., Sumathi, S., 2020. Multi-Functional Biological Effects of PdNPs Synthesized Using Agaricus bisporus. J. Clust Sci. 31, 391–400.

Nugroho, F.A.A., Iandolo, B., Wagner, J.B., Langhammer, C., 2016. Bottom-up nanofabrication of supported noble metal alloy nanoparticle arrays for plasmonics. ACS Nano 10, 2871–2879.

Rabiee, N., Bagherzadeh, M., Kiani, M., Ghadiri, A.M., 2020. Rosmarinus officinalis directed palladium nanoparticle synthesis: Investigation of potential antibacterial, antifungal and Mizoroki-Heck catalytic activities. Adv. Powder Technol. 15, 3983–3999.

Parasuraman, P., Antony, A.P., B, S.L.S., Sharan, A., Siddhardha, B., Kasinathan, K., Bahkali, N.A., Dawoud, T.M.S., Syed, A., 2019. Needa A Bahkali, Turki MS Dawoud, Asad Syed, Antimicrobial photodynamic activity of toluidine blue encapsulated in mesoporous silica nanoparticles against Pseudomonas aeruginosa and Staphylococcus aureus. Biofouling 35 (1), 89–103.

Ramesh, R., Yamini, V., Sundaram, S.J., Khan, F.L.A., Kaviyarasu, K., 2021. Investigation of structural and optical properties of NiO nanoparticles mediated by Plectranthus amboinicus leaf extract. Mater. Today:. Proc. 36, 268–272.

Badineni, V., Maseed, H., Arla, S.K., Yerramala, S., Naidu, B.V.K., Kaviyarasu, K., 2021. Effect of PVA/PVP protective agent on the formation of silver nanoparticles and its photocatalytic and antimicrobial activity. Mater. Today:. Proc. 36, 121–125.

Nithiyavathi, R., John Sundaram, S., Theophil Anand, G., Raj Kumar, D., Dhayal Raj, A., Al, D.A., Farraj, R.M., Aljowaie, M.R., AbdelGawwad, Y., Samson, K.K., 2021. Gum mediated synthesis and characterization of CuO nanoparticles towards infectious disease-causing antimicrobial resistance microbial pathogens. J. Infect. Public Health 14 (12), 1893–1902.

Ramesh, R., Catherine, G., Sundaram, S.J., Khan, F.L.A., Kaviyarasu, K., 2021. Synthesis of Mn_3O_4 nano complex using aqueous extract of Helianthus annuus seed cake and its effect on biological growth of Vigna radiata. Mater. Today:. Proc. 36, 184–191.

Saldan, I., Semenyuk, Y., Marchuk, I., Reshetnyak, O., 2015. Chemical synthesis and application of palladium nanoparticles. J. Mater. Sci. 24, 88–97.

Saldan, I., Semenyuk, Y., Marchuk, I., Reshetnyak, O., 2015. Chemical synthesis and application of palladium nanoparticles. J. Mater. Sci. 50, 2337–2354.

Salem, S.S., Fouda, A., 2021. Green synthesis of metallic nanoparticles and their prospective biotechnological applications: an overview. Biol. Trace Elem. Res. 199, 344–370.

Thakkar, K.N., Mhatre, S.S., Parikh, R.Y., 2010. Biological synthesis of metallic nanoparticles. Nanomed. J. 6, 257–262.

Mangala Nagasundari, S., Muthu, K., Kaviyarasu, K., Farraj, D.A.A., Alkufeidy, R.M., 2021. Current trends of Silver doped Zinc oxide nanowires photocatalytic degradation for energy and environmental application. Surf. Interfaces 23.

Thirupathy, C., Lims, S.C., Sundaram, S.J., Mahmoud, A.H., Kaviyarasu, K., 2020. Equilibrium synthesis and magnetic properties of $BaFe_{12}O_{19}/NiFe_2O_4$ nanocomposite prepared by co precipitation method. J. King Saud Univ.-Sci. 32 (2), 1612–1618.

Geetha, N., Sivaranjani, S., Ayeshamariam, A., Siva Bharathy, M., Nivetha, S., Kaviyarasu, K., Jayachandran, M., 2018. High performance photo-catalyst based on nanosized ZnO - TiO_2 nanoplatelets for removal of RhB under visible light irradiation. J. Adv. Microsc. Res. 13 (1), 12–19.

Amanulla, A.M., Sundaram, R., Kaviyarasu, K., 2019. An investigation of structural, magnetical, optical, antibacterial and humidity sensing of Zr (MoO4) 2-ZrO2 nanocomposites. Surf. Interfaces 16, 132–140.

Subbareddy, Y., Kumar, R.N., Sudhakar, B.K., Reddy, K.R., Martha, S.K., Kaviyarasu, K., 2020. A facile approach of adsorption of acid blue 9 on aluminium silicate-coated Fuller's Earth - Equilibrium and kinetics studies. Surf. Interfaces 19.

Alhaji, N.M.I., Nathiya, D., Kaviyarasu, K., Meshram, M., Ayeshamariam, A., A., 2019. comparative study of structural and photocatalytic mechanism of AgGaO2 nanocomposites for equilibrium and kinetics evaluation of adsorption parameters. Surf. Interfaces 17, 100375.

George, A., Magimai Antoni Raj, D., Venci, X., Dhayal Raj, A., Albert Irudayaraj, A., Josephine, R.L., John Sundaram, S., Al-Mohaimeed, A.M., Al Farraj, D.A., Chen, T.-W., Kaviyarasu, K., 2022. Photocatalytic effect of CuO nanoparticles flower-like 3D nanostructures under visible light irradiation with the degradation of methylene blue (MB) dye for environmental application. Environ. Res. 203.

Magdalane, C.M., Priyadharsini, G.M.A., Kaviyarasu, K., Jothi, A.I., Simiyon, G.G., 2021. Synthesis and characterization of TiO2 doped cobalt ferrite nanoparticles via microwave method: investigation of photocatalytic performance of congo red degradation dye. Surf. Interfaces 25.

Amanulla, A.M., Magdalane, C.M., Saranya, S., Sundaram, R., Kaviyarasu, K., 2021. Selectivity, stability and reproducibility effect of CeM-CeO2 modified PIGE electrode for photoelectrochemical behaviour of energy application. Surf. Interfaces 22.

Kayalvizhi, K., Alhaji, N.M.I., Saravanakkumar, D., Mohamed, S.B., Kaviyarasu, K., Ayeshamariam, A., Al-Mohaimeed, A.M., AbdelGawwad, M.R., Elshikh, M.S., 2022. Adsorption of copper and nickel by using sawdust chitosan nanocomposite beads - A kinetic and thermodynamic study. Environ. Res. 203.

Perumal, V., Inmozhi, C., Uthrakumar, R., Robert, R., Chandrasekar, M., Mohamed, S. B., Honey, S., Raja, A., Al-Mekhlafi, F.A., Kaviyarasu, K., 2022. Enhancing the photocatalytic performance of surface-Treated SnO2 hierarchical nanorods against methylene blue dye under solar irradiation and biological degradation. Environ. Res. 209.

George, A., Dhayal Raj, A., Albert Irudayaraj, A., Josephine, R.L., Venci, X., John Sundaram, S., Rajakrishnan, R., Kuppusamy, P., Kaviyarasu, K., 2022. Regeneration study of MB in recycling runs over nickel vanadium oxide by solvent extraction for photocatalytic performance for wastewater treatments. Environ. Res. 211.

Ayeshamariam, A., Kaviyarasu, K., Alhaji, N.M.I., Kavin Micheal, M., Jayachandran, M., 2021. In: Applications of Advanced Green Materials. Elsevier, pp. 373–394.

Ramasubba ReddyPalem, Ganesh Shimoga, Sang-YounKim, ChinnaBathula, Gajanan S.Ghodake, Soo-HongLe, Biogenic palladium nanoparticles: An effectual environmental benign catalyst for organic coupling reactions, Journal of Industrial and Engineering Chemistry, 106, 52-68, 2022.

Bathula, C., K, S., Kumar K, A., Yadav, H., Ramesh, S., Shinde, S., Shrestha, N.K., Mallikarjuna, K., Kim, H., 2020. Haekyoung Kim, Ultrasonically driven green synthesis of palladium nanoparticles by Coleus amboinicus for catalytic reduction and Suzuki-Miyaura reaction. Colloids Surf., B 192.

Mallikarjuna, K., Bathula, C., Dinneswara Reddy, G., Shrestha, N.K., Kim, H., Noh, Y.-Y., 2019. Au-Pd bimetallic nanoparticles embedded highly porous Fenugreek polysaccharide based micro networks for catalytic applications. Int. J. Biol. Macromol. 126, 352–358.

Mallikarjuna, K., Bathula, C., Buruga, K., Shrestha, N.K., Noh, Y.-Y., Kim, H., 2017. Green synthesis of palladium nanoparticles using fenugreek tea and their catalytic applications in organic reactions. Mater. Lett. 205, 138–141.